Yuan Cheng[1]
Institute of High Performance Computing,
A*STAR,
Singapore 138632
e-mail: chengy@ihpc.a-star.edu.sg

Nicola Maria Pugno
Department of Civil, Environmental and
Mechanical Engineering,
University of Trento,
Via Mesiano 77,
I-38123 Trento, Italy

Xinghua Shi
State Key Laboratory of Nonlinear Mechanics,
Institute of Mechanics,
Chinese Academy of Sciences,
Beijing 100190, China

Bin Chen
Department of Engineering Mechanics,
Zhejiang University,
Hangzhou 310027, China

Huajian Gao[1]
School of Engineering,
Brown University,
610 Barus & Holley,
182 Hope Street,
Providence, RI 02912
e-mail: huajian_gao@brown.edu

Surface Energy-Controlled Self-Collapse of Carbon Nanotube Bundles With Large and Reversible Volumetric Deformation

Molecular dynamics simulations are performed to investigate the effect of surface energy on equilibrium configurations and self-collapse of carbon nanotube bundles. It is shown that large and reversible volumetric deformation of such bundles can be achieved by tuning the surface energy of the system through an applied electric field. The dependence of the bundle volume on surface energy, bundle radius, and nanotube radius is discussed via a dimensional analysis and determined quantitatively using the simulation results. The study demonstrates potential of carbon nanotubes for applications in nanodevices where large, reversible, and controllable volumetric deformations are desired.
[DOI: 10.1115/1.4024174]

Keywords: molecular dynamics, carbon nanotube bundle

1 Introduction

A key promise of nanotechnology is to establish an unprecedented capability to tailor design materials with superior properties via controlled assembly of nanostructures, such as graphene sheets [1–4] and carbon nanotubes (CNTs) [5–11]. During such assembly, an interesting feature of single-walled carbon nanotubes (SWCNTs) and multiwalled carbon nanotubes (MWCNTs) is that they can self-collapse due to intra- or intertube van der Waals interactions. For example, Xiao et al. [12] investigated the collapse of SWCNTs and MWCNTs using the so-called atomic-finite element method and showed that the collapse behaviors of a MWCNT depends on the number of walls and the radius of the innermost wall. There exists a critical diameter for self-collapse of such tubes into a partially collapsed "dog-bone" configuration. Elliott et al. [13] performed molecular dynamics (MD) simulations of the size-dependent collapse of SWCNT bundles under pressure and identified a critical collapse diameter between 4.16 nm and 6.94 nm under the atmospheric pressure. The related theory indicates that the self-collapse can increase the strength of a SWCNT bundle [14].

It has been recently reported that the effective surface energy of carbon nanoscrolls can be tuned through an applied DC/AC electric field and used to control the radius of their hollow inner cores [15], leading to possible applications as controllable water channels and nano-oscillators [15,16]. In a previous work from our group, the effect of an applied electric field on carbon nanoscrolls was represented by an effective surface energy, γ_{eff} [16]. When an external electric field is applied along the axial direction of the carbon nanoscrolls, the effective surface energy, γ_{eff}, can be calculated as $\gamma_{\mathrm{eff}} = \gamma_{vdW} + \gamma_{\mathrm{dipole}}$. Here, γ_{vdW} is the surface energy due to the van der Waals interaction between carbon atoms and γ_{dipole} is the dipole-dipole interaction-induced surface energy. The polarization of carbon atoms could significantly alter the effective surface energy of carbon nanoscrolls [16].

Earlier studies have also shown that electric fields on carbon nanotubes can induce polarization of carbon atoms in sp2 structures [17] and deformation of the CNTs [18]. Therefore, we can regard the effective surface energy as composed of contributions from both the van der Waals and dipole-dipole interactions. The effective surface energy of carbon nanotubes can be controlled via an applied electric field.

In the present paper, we investigate this issue via MD simulations of SWCNT bundles under different prescribed values of surface energy. We will investigate the self-collapse and subsequent recovery of SWCNT bundles as the surface energy is raised above the critical value and dropped down again. Such surface energy-controlled deformation mechanism with large and reversible volumetric changes suggests possible applications of CNT bundles in nanoactuators and artificial muscles.

2 Methods

Figure 1 shows the simulation system of a bundle of seven (42,42) SWCNTs, hereafter referred to as bundle I, in which each tube has diameter of 5.70 nm and length of 2.50 nm. The chosen diameter falls within the range from 4.16 nm to 6.94 nm required for self-collapse under atmospheric pressure. All simulations are carried out using MD simulation package Large-scale Atomic/Molecular Massively Parallel Simulator [19]. The simulations are

[1]Corresponding author.
Manuscript received December 27, 2012; final manuscript received February 4, 2013; accepted manuscript posted April 10, 2013; published online May 31, 2013. Editor: Yonggang Huang.

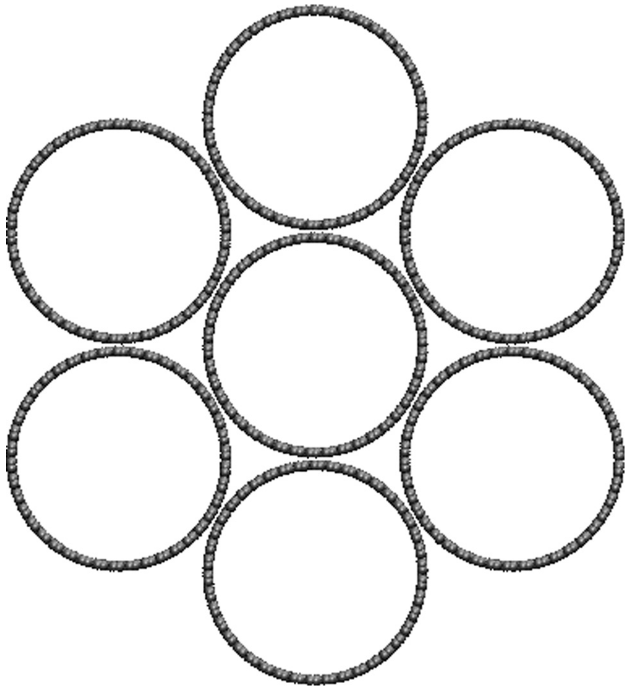

Fig. 1 Initial configuration of a bundle of seven single-walled carbon nanotubes (bundle I)

performed at 10 K after 2000 steps of energy minimization based on the conjugate gradient method. A time step of 0.001 ps is used with a microcanonical NVE ensemble. Periodic boundary conditions are imposed along the axial direction of the CNTs. The adaptive intermolecular reactive bond order (AIREBO) potential [20], which is widely used in the investigations of thermal and mechanical properties of carbon nanomaterials, such as CNTs and graphene [21–23], is adopted to describe breaking and creation of covalent bonds with associated changes in hybridization of atomic orbitals within a classical potential. Nonbonded interactions among carbon atoms on the CNTs are described by the Lennard–Jones (L–J) potential $\mathrm{U} = 4\varepsilon'_{\mathrm{cc}}\left[(\sigma/\mathrm{r_{ij}})^{12} - (\sigma/\mathrm{r_{ij}})^{6}\right]$. In the L–J potential, $\varepsilon'_{\mathrm{cc}}$ is the depth of the potential well and $\sigma = 0.34\mathrm{nm}$ is the distance at which the L–J potential vanishes. Tuning surface energy will change the strength of interlayer interaction rather than the interlayer distance. Therefore, the energy well-depth $\varepsilon'_{\mathrm{cc}}$ is a suitable tuning parameter of surface energy in MD. The simulations are based on a microcanonical NVE ensemble with time step of 0.001 ps. The cut-off distances for nonbonded interactions follow the default values in AIREBO potential, ranging from 1.7 nm to 2.0 nm [20].

The L–J well depth ε'_{cc} is initially set at the default value of $\varepsilon_{cc} = 0.2740\ \mathrm{kJ/mol}$ in the AIREBO potential and then increased in a step-wise manner in the simulations to mimic the effect of an increasing electric field [16]. At each step, a particular parameter ε'_{cc} is adopted and the simulation run for 500 ps until the system reaches equilibrium.

3 Dimensional Analysis

In order to organize the simulation results, we note the following system parameters of interest: the volume V of the SWCNT bundle per unit length, the van der Waals length parameter σ, the radius R of each tube, the radius D of the circumscribed circle of the bundle, the surface energy γ, and the bending modulus κ of graphene. The bending energy and surface energy per unit area of graphene can be expressed as $U_B = \kappa/2R^2$ and $U_s = \gamma \propto \varepsilon'_{cc}/\sigma^2$, respectively. Therefore, the ratio between the bending and surface energies could be expressed as $\lambda = \varepsilon'_{cc}R^2/\kappa\sigma^2$ [14].

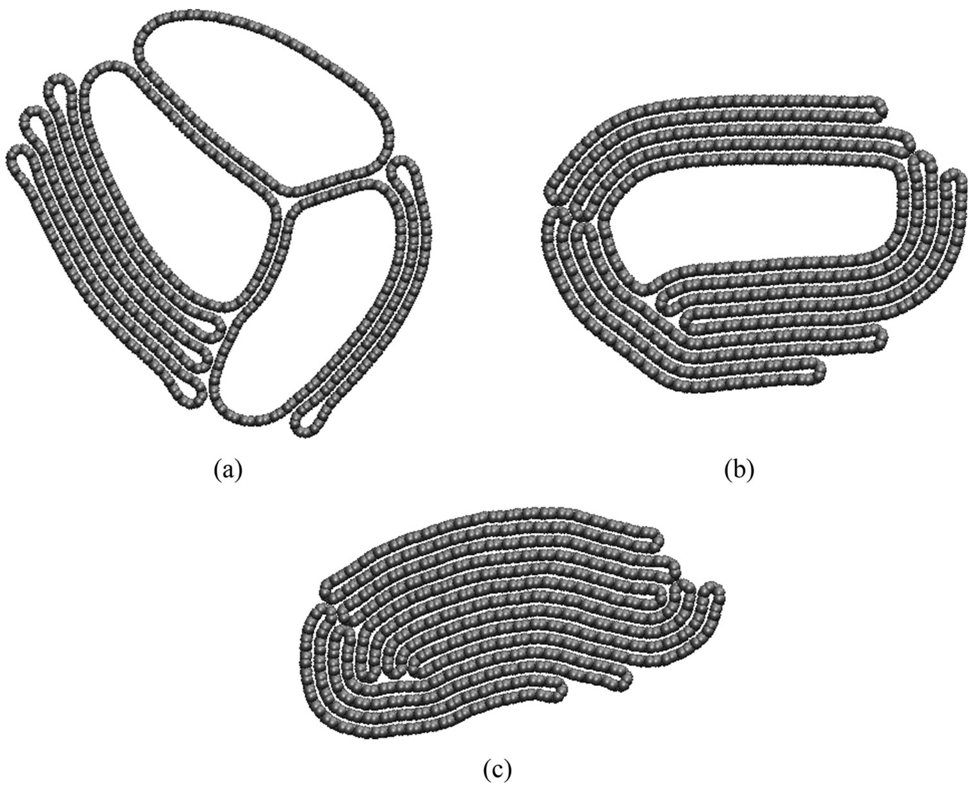

Fig. 2 Snapshot configurations of carbon nanotube bundle I at 500 ps under increasing values of surface energy determined by the van der Waals potential well depth: (*a*) $\varepsilon'_{cc} = \varepsilon_{cc}$, (*b*) $\varepsilon'_{cc} = 4\varepsilon_{cc}$, or (*c*) $\varepsilon'_{cc} = 6\varepsilon_{cc}$

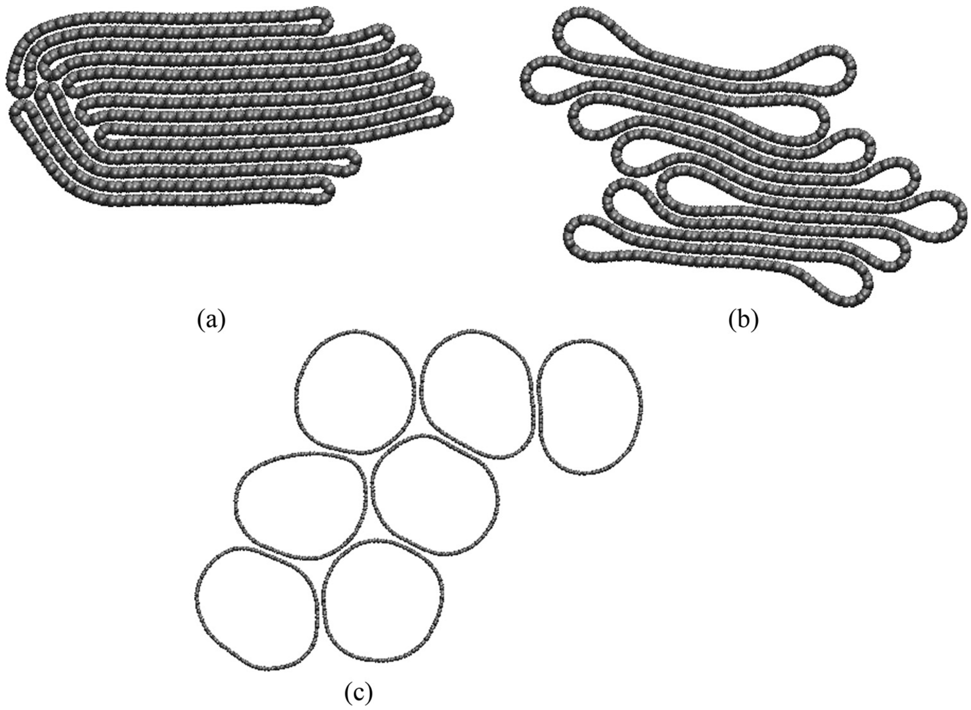

Fig. 3 Snapshot configurations of bundle I at 500 ps under decreasing values of surface energy determined by the van der Waals potential well depth: (*a*) $\varepsilon'_{cc} = 2\varepsilon_{cc}$, (*b*) $\varepsilon'_{cc} = 0.4\varepsilon_{cc}$, or (*c*) $\varepsilon'_{cc} = 0.2\varepsilon_{cc}$

Among the above system parameters, we can identify the following dimensionless parameters: $\tilde{V} = V/D^2$, $\tilde{\varepsilon}' = \varepsilon'_{cc}/\kappa$, $\tilde{\varepsilon} = \varepsilon_{cc}/\kappa$, $\tilde{R} = R/\sigma$, and $\tilde{D} = D/R$. Therefore, the bundle volume (per unit axial length) could be expressed as $\tilde{V} = f(\tilde{\varepsilon}', \tilde{\varepsilon}, \tilde{R}, \tilde{D})$. For the present problem, since ε_{cc} and κ are fixed, it will be most convenient to express $\tilde{V}$ in terms of a relative change of surface energy $\Delta\tilde{\varepsilon} = (\varepsilon'_{cc} - \varepsilon_{cc})/\varepsilon_{cc}$ (i.e., $\tilde{V} = f(\Delta\tilde{\varepsilon}, \tilde{R}, \tilde{D})$).

4 Results

4.1 Self-Collapse and Recovery of CNT Bundle I. Figure 2 shows representative snapshots depicting the self-collapse of bundle I as $\Delta\tilde{\varepsilon} = (\varepsilon'_{cc} - \varepsilon_{cc})/\varepsilon_{cc}$ is increased in a stepwise manner from its default value of zero. For each current value of $\Delta\tilde{\varepsilon}$, the mean value of the equilibrium bundle volume per unit axial length is recorded, and the equilibrium structure is then used as the initial configuration for the next value of $\Delta\tilde{\varepsilon}$. The bundle is seen to undergo partial (Figs. 2(*a*) and 2(*b*)) or complete (Fig. 2(*c*)) collapse as $\Delta\tilde{\varepsilon}$ is increased from 0 to 5. Note that the SWCNTs in the bundle do not collapse simultaneously; this behavior is caused by different loading conditions each tube is subject to. For example, the SWCNT in the center is compressed by adjacent tubes from different directions in a relatively symmetric way. In comparison, the SWCNTs in the outer layer are loaded asymmetrically by lateral and inner tubes. Therefore, the SWCNTs in the bundle do not collapse simultaneously. Upon reduction in $\Delta\tilde{\varepsilon}$, the self-collapse of the CNT bundle can be reversed and the initial volume recovered. Figure 3 shows representative snapshots of the equilibrium bundle configuration as $\Delta\tilde{\varepsilon}$ is reduced from that of a fully collapsed state to $\Delta\tilde{\varepsilon} = 1$, -0.6, and -0.8. At $\Delta\tilde{\varepsilon} = 1$, the collapsed CNTs start to open into "dog-bone" configurations [12]. As $\tilde{\varepsilon}$ is further reduced to -0.6, the bundle expands to a partially collapsed configuration with substantial gain in volume. At $\Delta\tilde{\varepsilon} = -0.8$, more than 95% of the initial volume of the CNT bundle shown in Fig. 1 is recovered. In this way, a large and reversible volumetric deformation of the CNT bundle has been achieved through the surface energy controlled self-collapse and re-expansion.

4.2 Bundle Volume $\tilde{V}$ Versus Surface Energy Parameter $\Delta\tilde{\varepsilon}$. With the bending modulus of graphene estimated at $\kappa = 0.17$ nNnm [19], the normalized bundle volume $\tilde{V}$ could be plotted as a function of the surface energy parameter $\Delta\tilde{\varepsilon}$ for different values of $\tilde{R}$ and $\tilde{D}$, as shown in Fig. 4. It is shown that, for bundle I, with increasing surface energy, the volume of the bundle decreases until full collapse occurs at a critical value of $\Delta\tilde{\varepsilon}$; if the surface energy is reduced subsequently, the bundle volume can recover from that of the fully collapsed state to a value close to the initial state, resulting in a hysteretic behavior due to variations in the van der Waals interaction between opposing walls of the collapsed CNTs.

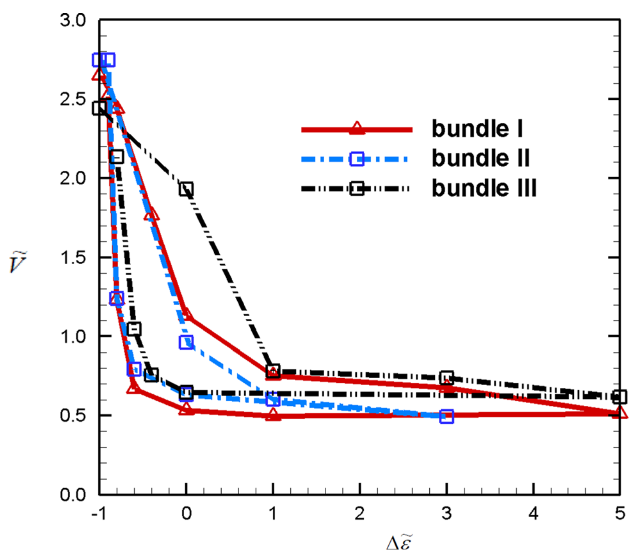

Fig. 4 Normalized bundle volume $\tilde{V}$ as a function of normalized surface energy change $\Delta\tilde{\varepsilon}$

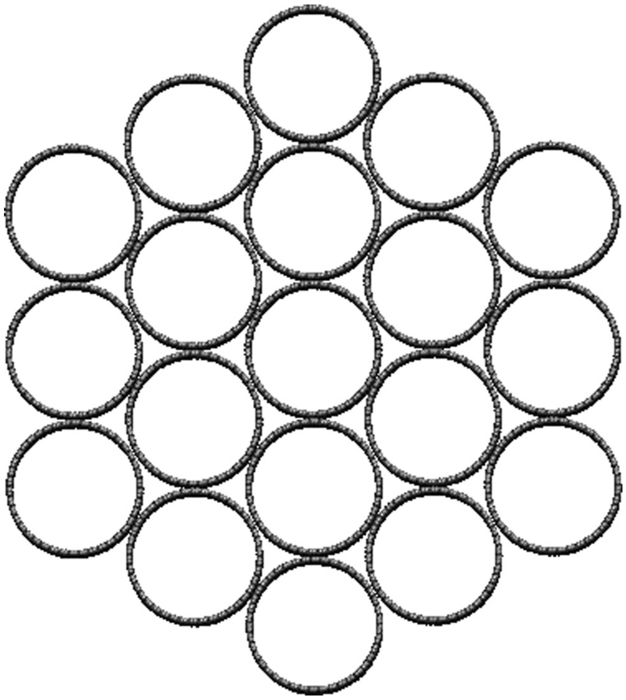

Fig. 5 Initial configuration of a bundle of 19 single-walled carbon nanotubes (bundle II)

To investigate the effect of the normalized bundle size $\tilde{D}$, we repeat the simulations for a larger CNT bundle, referred to as bundle II. This bundle is constructed by adding an additional layer of SWCNTs around bundle I, leading to a total of 19 same-sized SWCNTs, as shown in Fig. 5. The CNT bundle is again observed to collapse under increasing $\Delta\tilde{\varepsilon}$ and recover upon decreasing $\Delta\tilde{\varepsilon}$, similar to the behavior of bundle I. The fully collapsed configuration of bundle II is shown in Fig. 6.

To investigate the effect of the normalized tube size $\tilde{R}$, we repeat the simulations for another CNT bundle, referred to as bundle III, which has the same configuration as bundle I but with smaller SWCNTs of type (30,30) with radius roughly $1/\sqrt{2}$ of those in bundle I.

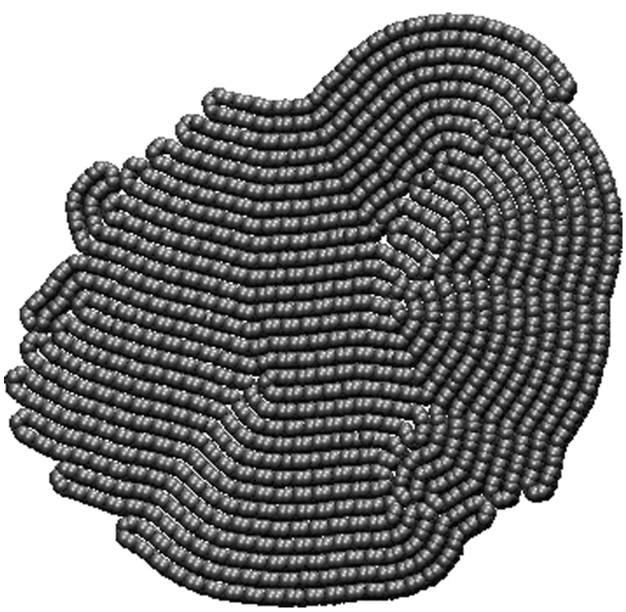

Fig. 6 Fully collapsed configuration of carbon nanotube bundle II

As shown in Fig. 4, the three bundles under investigation exhibit similar $\tilde{V} = f(\Delta\tilde{\varepsilon}, \tilde{R}, \tilde{D})$ curves in response to variations in $\Delta\tilde{\varepsilon}$. Bundle III shows a more pronounced hysteresis behavior than the other two bundles, while the hysteresis behaviors of bundle I and II almost overlap when $\Delta\tilde{\varepsilon} < 0$. Compared with bundle I and bundle II, bundle III has a smaller tube radius, indicating that the collapse-recovery behavior is affected more by the tube size than the bundle size. Similar observation was reported in an earlier work that self-collapse of CNT bundle is determined by the radius of SWCNTs [13], which is also in agreement with an analysis given in Ref. [14].

The dimensionless analysis suggests that, at small SWCNT radii, the energy barrier for tube collapse is higher, and a stronger surface energy is required to collapse the tube, subsequently causing more pronounced hysteresis.

5 Conclusion

In summary, we have investigated via MD simulations the self-collapse and recovery of CNT bundles with large and reversible volumetric deformation. Our simulations indicate that the volume of the bundle can be controlled by tuning the effective surface energy of the system, which in practice can be accomplished by an applied electric field.

Acknowledgment

The work reported has been supported by the A*Star Visiting Investigator Program "Size Effects in Small Scale Materials" hosted at the Institute of High Performance Computing in Singapore. N.M.P. acknowledges funding from the European Research Council under the European Union's Seventh Framework Programme (FP7/2007-2013)/ERC Grant Agreement No. (279985) (ERC StG 2011 to N.M.P. on "Bio-inspired hierarchical super nanomaterials").

References

[1] Novoselov, K. S., Geim, A. K., Morozov, S. V., Jiang, D., Zhang, Y., Dubonos, S. V., Grigorieva, I. V., and Firsov, A. A., 2004, "Electric Field Effect in Atomically Thin Carbon Films," Science, **306**, pp. 666–669.

[2] Berger, C., Song, Z., Li, X., Wu, X., Brown, N., Naud, C., Mayou, D., Li, T., Hass, J., Marchenkov, A. N., Conrad, E. H., First, P. N., and de Heer, W. A., 2006, "Electronic Confinement and Coherence in Patterned Epitaxial Graphene," Science, **312**, pp. 1191–1196.

[3] Stankovich, S., Dikin, D. A., Dommett, G. H. B., Kohlhaas, K. M., Zimney, E. J., Stach, E. A., Piner, R. D., Nguyen, S. T., and Ruoff, R. S., 2006, "Graphene-Based Composite Materials," Nature, **442**, pp. 282–286.

[4] Dikin, D. A., Stankovich, S., Zimney, E. J., Piner, R. D., Dommett, G. H. B., Evmenenko, G., Nguyen, S. T., and Ruoff, R. S., 2007, "Preparation and Characterization of Graphene Oxide Paper," Nature, **448**, pp. 457–460.

[5] Zhang, M., Atkinson, K. R., and Baughman, R. H., 2004, "Multifunctional Carbon Nanotube Yarns by Downsizing an Ancient Technology," Science, **306**, pp. 1358–1361.

[6] Zhu, H. W., Xu, C. L., Wu, D. H., Wei, B. Q., Vajtai, R., and Ajayan, P. M., 2002, "Direct Synthesis of Long Nanotube Strands," Science, **296**, pp. 884–886.

[7] Jiang, K., Li, Q., and Fan, S., 2002, "Nanotechnology: Spinning Continuous Carbon Nanotube Yarns," Nature, **419**, p. 801.

[8] Dalton, A. B., Collins, S., Muñoz, E., Razal, J. M., Ebron, V. H., Ferraris, J. P., Coleman, J. N., Kim, B. G., and Baughman R. H., 2003, "Super-Tough Carbon-Nanotube Fibres," Nature, **423**, p. 703.

[9] Koziol, K., Vilatela, J., Moisala, A., Motta, M., Cunniff, P., Sennett, M., and Windle, A., 2007, "High-Performance Carbon Nanotube Fiber," Science, **318**, pp. 1892–1895.

[10] Salvato, M., Cirillo, M., Lucci, M., Orlanducci, S., Ottaviani, I., Terranova, M. L., and Toschi, F., 2012, "Macroscopic Effects of Tunnelling Barriers in Aggregates of Carbon Nanotube Bundles," J. Phys. D: Appl. Phys., **45**, p. 105306.

[11] Hisashi, A., Tetsutaroh, K., and Katsumi, Y., 2002, "Preparation of Straight Multiwalled Carbon Nanotube Bundles," J. Phys. D: Appl. Phys., **35**, pp. 1076–1079.

[12] Xiao, J., Liu, B., Huang, Y., Zuo, J., Hwang, K.-C., and Yu, M.-F., 2007, "Collapse and Stability of Single and Multi-Wall Carbon Nanotubes," Nanotechnology, **18**, p. 395703.

[13] Elliott, J. A., Sandler, J. K. W., Windle, A. H., Young, R. J., and Shaffer, M. S. P., 2004, "Collapse of Single-Wall Carbon Nanotubes is Diameter Dependent," Phys. Rev. Lett., **92**, p. 095501.
[14] Pugno, N. M., 2010, "The Design of Self-Collapsed Super-Strong Nanotube Bundles," J. Mech. Phys. Solids, **58**, pp. 1397–1410.
[15] Shi, X., Cheng, Y., Pugno, N. M., and Gao, H., 2010, "A Translational Nanoactuator Based on Carbon Nanoscrolls on Substrates," Appl. Phys. Lett., **96**, pp. 517–521.
[16] Shi, X., Cheng, Y., Pugno, N. M., and Gao, H., 2010, "Tunable Water Channels With Carbon Nanoscrolls," Small, **6**, pp. 739–744.
[17] Langlet, R., Devel, M., and Lambin, Ph., 2006, "Computation of the Static Polarizabilities of Multi-Wall Carbon Nanotubes and Fullerites Using a Gaussian Regularized Point Dipole Interaction Model," Carbon, **44**, pp. 2883–2895.
[18] Wang, Z., and Devel, M., 2007, "Electrostatic Deflections of Cantilevered Metallic Carbon Nanotubes Via Charge-Dipole Model," Phys. Rev. B, **76**, p. 195434.
[19] Plimpton, S., 1995, "Fast Parallel Algorithms for Short-Range Molecular Dynamics," J. Comp. Phys., **117**, pp. 1–19.
[20] Stuart, S. J., Tutein, A. B., and Harrison, J. A., 2000, "A Reactive Potential for Hydrocarbons With Intermolecular Interactions," J. Chem. Phys., **112**, pp. 6472–6486.
[21] Brenner, D. W., Shenderova, O. A., Harrison, J. A., Stuart, S. J., Ni, B., and Sinnott, S. B., 2002, "A Second-Generation Reactive Empirical Bond Order (REBO) Potential Energy Expression for Hydrocarbons," J. Phys.: Condens. Matter, **14**, pp. 783–802.
[22] Zhang, Y. Y., Wang, C. M., Cheng, Y., and Xiang, Y., 2011, "Mechanical Properties of Bilayer Graphene Sheets Coupled by sp^{+} Bonding," Carbon, **49**, pp. 4511–4517.
[23] Pei, Q. X., Sha, Z. D., and Zhang, Y. W., 2011, "A Theoretical Analysis of the Thermal Conductivity of Hydrogenated Graphene," Carbon, **49**, pp. 4752–4759.